Research Article

Hydrogen-rich water ameliorates neuropathological impairments in a mouse model of Alzheimer's disease through reducing neuroinflammation and modulating intestinal microbiota

https://doi.org/10.4103/1673-5374.317992

Date of submission: October 8, 2020

Date of decision: November 19, 2020

Date of acceptance: March 18, 2021

Date of web publication: July 8, 2021

Yi-Tong Lin[1, #], Qing-Qing Shi[1, #], Lei Zhang[1, #], Cai-Ping Yue[1], Zhi-Jun He[1], Xue-Xia Li[1], Qian-Jun He[2], Qiong Liu[1], Xiu-Bo Du[1, 3, *]

Graphical Abstract

Hydrogen-rich water (HRW) prevents against Alzheimer's disease by improving the bioenergetics, modulating intestinal microbiota and inhibiting inflammation

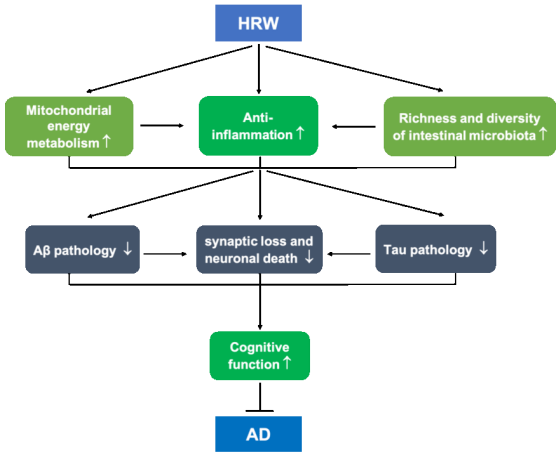

Abstract

Hydrogen exhibits the potential to treat Alzheimer's disease. Stereotactic injection has been previously used as an invasive method of administering active hydrogen, but this method has limitations in clinical practice. In this study, triple transgenic (3×Tg) Alzheimer's disease mice were treated with hydrogen-rich water for 7 months. The results showed that hydrogen-rich water prevented synaptic loss and neuronal death, inhibited senile plaques, and reduced hyperphosphorylated tau and neurofibrillary tangles in 3×Tg Alzheimer's disease mice. In addition, hydrogen-rich water improved brain energy metabolism disorders and intestinal flora imbalances and reduced inflammatory reactions. These findings suggest that hydrogen-rich water is an effective hydrogen donor that can treat Alzheimer's disease. This study was approved by the Animal Ethics and Welfare Committee of Shenzhen University, China (approval No. AEWC-20140615-002) on June 15, 2014.
Key Words: Alzheimer's disease; amyloid-β; anti-inflammation; bioenergetics; gut microbiota; hydrogen therapy; neurodegenerative disease; neurofibrillary tangles

Chinese Library Classification No. R453; R741.05; R378.2

Introduction

Although Alzheimer's disease (AD) was identified more than 100 years ago, an effective treatment strategy currently remains lacking (Frere and Slutsky, 2018; Jack et al., 2018). The main pathological features of AD are senile plaques and neurofibrillary tangles (NFTs), which are formed by amyloid-β (Aβ) aggregates and hyperphosphorylated tau, respectively. In addition, oxidative stress, inflammatory responses, and autophagic abnormalities also contribute to the pathogenesis of AD (Markesbery, 1997; Mostafavi et al., 2018; Fang et al., 2019). Accumulating evidence suggests that neuroinflammation plays an active role in the development of AD (Park et al., 2018; Ozben and Ozben, 2019; Gray et al., 2020). Epidemiological data have revealed that non-steroidal anti-inflammatory drugs may decrease the incidence of AD (Daniels et al., 2016). However, other studies have demonstrated that non-steroidal anti-inflammatory drugs may aggravate conditions in AD or increase the risk of this disease

[1]College of Life Sciences and Oceanography, Guangdong Provincial Key Laboratory for Plant Epigenetics, Shenzhen University, Shenzhen, Guangdong Province, China; [2]Guangdong Provincial Key Laboratory of Biomedical Measurements and Ultrasound Imaging, National-Regional Key Technology Engineering Laboratory for Medical Ultrasound, School of Biomedical Engineering, Health Science Center, Shenzhen University, Shenzhen, Guangdong Province, China; [3]Shenzhen Bay Laboratory, Shenzhen, Guangdong Province, China

*Correspondence to: Xiu-Bo Du, PhD, duxiubo@szu.edu.cn.

https://orcid.org/0000-0003-4907-074X (Xiu-Bo Du)

#These authors contributed equally to this work.

Funding: *This study was supported by the National Natural Science Foundation of China, No. 21771126 (to XBD); and the Shenzhen Bureau of Science, Technology and Information of China, No. JCYJ20180305124000597 (to XBD).*

How to cite this article: *Lin YT, Shi QQ, Zhang L, Yue CP, He ZJ, Li XX, He QJ, Liu Q, Du XB (2022) Hydrogen-rich water ameliorates neuropathological impairments in a mouse model of Alzheimer's disease through reducing neuroinflammation and modulating intestinal microbiota. Neural Regen Res 17(2):409-417.*

(Sehajpal et al., 2018). It is therefore necessary to develop effective anti-inflammatory AD drugs with low toxicity.

Hydrogen molecules are a special kind of antioxidant. As a gas molecule, hydrogen possesses the advantages of easy diffusion, fast action, and no obvious adverse reactions (Ohta, 2015; Iida et al., 2016). Furthermore, it is regarded as a promising potential therapy for many inflammation-related diseases, including neurodegenerative diseases, cancer, stroke, and ischemic injury (Iida et al., 2016; Yang et al., 2018; Zhang et al., 2019). Hydrogen has therefore been suggested as another important biologically active gas molecule, after nitric oxide, hydrogen sulfide, and carbon monoxide (Zhang and Bian, 2014; Olas, 2017; Kumar and Sandhir, 2018; Corpas et al., 2019). Recently, we developed palladium hydride nanoparticles and delivered them to the brains of AD model mice using stereotactic injection. This treatment showed promising potential as an AD therapy by eliminating oxidative stress and alleviating mitochondrial dysfunction (Zhang et al., 2019). However, stereotactic brain injection is invasive. In the present study, we therefore investigated the effects of hydrogen-rich water (HRW) treatment, which is a safer and more convenient administration route for hydrogen, on AD pathology. We used HRW in a mouse model of AD and observed its therapeutic effects.

Materials and Methods

Ethics statement

All animal handling and experiments were performed in strict accordance with the institutional guidelines of Shenzhen University regarding experimental animal use, and were approved on June 15, 2014, by the Animal Ethics and Welfare Committee of Shenzhen University (approval No. AEWC-20140615-002). All procedures were conducted in accordance with the ethical standards of the National Institutes of Health Guide for the Care and Use of Laboratory Animals.

Animals and intervention

The HRW was gifted from Beijing Vitality Hydrogen Source Beverage Ltd. (Beijing, China), and the hydrogen concentration was greater than 1.6 parts per million. The triple transgenic (3×Tg)-AD model mice expressed the mutant human genes TauP301L and APPswe, and the mutant mouse gene PS1M146V. According to previous research on this mouse model (Oddo et al., 2003; Billings et al., 2005), Aβ begins to accumulate in the neurons at 4 months old, and gradually spreads outside the neurons. The accumulation of Aβ may cause neuronal dysfunction, which can lead to cognitive deficits. The 3×Tg-AD mice (n = 30, 25–30 g) and B6:129SF2/J (wild-type, WT) mice (n = 15, 25–30 g) were purchased from the Jackson Laboratory (Bar Harbor, ME, USA). To avoid the influences of sex and estrogen, three-month-old male mice only were used in the study. The 3×Tg-AD mice were randomly divided into 3×Tg-AD (AD; n = 15) and HRW-treated 3×Tg-AD (AD + HRW; n = 15) groups, and the B6:129SF2/J mice were used as controls (n = 15). After being trained with a time-limited water supply (water was only provided from 10:00 a.m. to 2:00 p.m. every day) for 30 days, the 3-month-old 3×Tg-AD mice in the AD + HRW group were given HRW for 7 months, while the mice in the AD group were treated with normal drinking water for 7 months.

Behavioral tests

The Morris water maze experiment was used to test the spatial learning and memory abilities of 10-month-old mice, as previously described (Xie et al., 2018). The entire experiment lasted for 8 days, and consisted of two parts: training (days 1 to 5) and testing (days 6 and 8). Each mouse was gently placed in the water in the first quadrant and was allowed 60 seconds to find the platform. If the mouse failed to find the platform within 60 seconds, it was gently guided to the platform and allowed to remain there for 10 seconds. The escape latency was recorded by a camera system. The probe tests, with the platform removed, were performed 24 and 72 hours after the final training trial to assess short- and long-term memory consolidation. During the tests, mice were released into the water from an identical point in the first quadrant and allowed to swim freely for up to 120 seconds. Time spent in the target quadrant (quadrant III) and the number of target crossings (i.e., the former platform site) were recorded. All tests were analyzed using an automatic water maze program (Water Maze MT-200, Taimeng Technology Co., Ltd., Chengdu, China). The open-field test was performed according to previous protocols (Hammer et al., 2014; Shoji et al., 2016) with a few modifications. A polyvinyl chloride box (100 cm × 100 cm × 40 cm) (Zhishu Duobao Biotechnology Co., Ltd., Beijing, China) with the bottom equally divided into 25 squares was used as the open field. During the test, each mouse was released into the center of the box and then allowed to explore for 3 minutes. Three parameters were collected: number of grids crossed (grids were only counted if all limbs of the mouse entered the grid), rearing frequency, and defecation frequency.

Sample collection

After the behavioral tests, mice were anaesthetized using isoflurane (Reward Life Technology Co., Ltd., Shenzhen, China). The mouse brains were then collected and soaked in phosphate-buffered saline (PBS) for 30 minutes before being divided into the left and right hemispheres. The hippocampus and cortex were dissected from the right hemisphere and stored at –80°C for the subsequent biochemical and western blot analyses. The other hemisphere was fixed in 4% phosphate-buffered paraformaldehyde for immunofluorescence, silver staining, and Nissl staining. In addition, the cecal contents (150–200 mg) were collected and frozen for the gut microbiota analysis.

Western blot analysis

Western blot analysis was performed to determine protein levels in the mouse hippocampus, as previously described (Xie et al., 2018). The blots were incubated with primary antibody overnight at 4°C, and were then incubated with horseradish peroxidase-conjugated secondary antibody for 2 hours at room temperature. All primary and secondary antibodies used in this study are summarized in **Additional Table 1**. Protein bands were visualized using the Image Station (Tanon-5200, Tanon Science & Technology Co., Ltd., Shanghai, China) using an enhanced chemiluminescence detection reagent. The band intensities of immunoblots were quantified using ImageJ software (National Institutes of Health, Bethesda, MD, USA).

Immunofluorescence, glycine silver staining, and Nissl staining

Brain tissue was fixed in 4% paraformaldehyde for 24 hours, cryopreserved overnight in graded sucrose solutions at 4°C, and embedded in optimal cutting temperature compound. Subsequently, the embedded tissue blocks were cut into 8 μm sections, which were mounted onto adhesive glass slides.

For immunofluorescence experiments, sections were rinsed with PBS, permeabilized with 2% Triton X-100, and blocked with 1% bovine serum albumin in PBS with Tween-20. Next, sections were incubated overnight at 4°C with primary antibodies, followed by incubation with Dylight 488/594-conjugated secondary antibodies for 1.5 hours at room temperature (**Additional Table 1**). After being washed with PBS with Triton X-100, the sections were stained with 4′,6-diamidino-2-phenylindole for 5 minutes and then sealed with anti-fluorescence quenching sealant (Beyotime, Shanghai, China). Finally, the images were captured using a confocal microscope (FV1000, Olympus Corporation, Tokyo, Japan). The Aβ, ionized calcium-binding adapter molecule 1

(Iba-1), and DAPI signals were evaluated using Image Pro Plus software (Media Cybernetics, Inc., Rockville, MD, USA), and the results were expressed as Aβ/DAPI or Iba-1/DAPI.

For the glycine sliver staining, sections were de-stained and sequentially treated with xylene, anhydrous ethanol, 75% ethanol, and water. The sections were subsequently stained in an acidic formaldehyde solution for 5 minutes and washed three times with distilled water. Thereafter, the sections were stained for 3–5 minutes with glycine silver solution that had been preheated to 37°C, and were then treated with reducing solution and washed with distilled water. Finally, the sections were observed using a confocal microscope (FV1000, Olympus Corporation). The NFT-positive areas were evaluated using Image Pro Plus software, and the results were expressed as the percentage of NFT-occupied area.

For Nissl staining, the sections were washed twice with PBS, dehydrated through an ethanol gradient, and immersed in xylene. After being stained with cresyl violet (0.5%) for 10 minutes, the sections were observed using a fluorescence microscope (BX51, Olympus Corporation). The Nissl-positive areas were assessed using Image Pro Plus software, and the results were expressed as the percentage of Nissl-positive area.

Adenosine triphosphate measurement

Adenosine triphosphate (ATP) levels in fresh hippocampal tissue were measured using an ATP assay kit (Beyotime). Each sample (20 mg) was homogenized in lysis buffer (150 μL; Beyotime) and centrifuged at 12,000 r/min for 5 minutes at 4°C. The collected supernatants were seeded into the wells of a 96-well plate containing ATP assay medium (100 μL). Subsequently, the relative light unit was determined using a luminometer (SpectraMAX 190 Microplate Reader, Molecular Devices, San Jose, CA, USA) and normalized against protein concentrations that were quantified using the bicinchoninic acid assay (Smith et al., 1985).

Gut microbiota analysis

The 16S ribosomal RNA gene was sequenced from cecal contents. The MetaVx Library Preparation kit (GENEWIZ, Inc., South Plainfield, NJ, USA) was used to prepare amplicon libraries. The DNA library was then evaluated using Bioanalyzer (Agilent Technologies, Palo Alto, CA, USA), and quantified with Qubit 2.0 Fluorometer (Thermo Fisher Scientific, Waltham, MA, USA). The 16S ribosomal RNA data analysis was performed using QIIME data analysis software (http://www.wernerlab.org/software/macqiime/citations). Quality filtering was executed to remove any low-quality sequences. Next, sequences with 97% similarity were quantified into operational taxonomic unit thresholds using the clustering program VSEARCH 1.9.6 (https://zenodo.org/record/44512). The taxonomy of the sequences was further determined using the Ribosomal Database Project Classifier (http://rdp.cme.msu.edu/classifier/classifier.jsp) at a minimum threshold of 0.8. With the analysis of operational taxonomic units, the α diversity indices Chao1 and Shannon were calculated using a random sampling method of sample sequence, and rarefaction curves were drawn. Unbiased UniFrac analysis (Lozupone and Knight, 2005) was used to determine whether there were significant differences in microbial communities between samples.

Statistical analysis

All data are expressed as the mean ± standard error of the mean (SEM). The significance level was established as $P < 0.05$. Statistical analyses were performed using one-way analysis of variance followed by Tukey's *post hoc* test with GraphPad Prism 8.0 (GraphPad Software Inc., San Diego, CA, USA).

Results

HRW improves cognitive impairment in 3×Tg-AD mice

To investigate the role of HRW in the learning and memory abilities of 3×Tg-AD mice, the Morris water maze test was performed after 7 months of HRW treatment. The 3×Tg-AD mice had difficulties in searching for the hidden platform compared with WT mice, and had chaotic and irregular swimming traces, suggesting that these mice have defective learning and memory abilities. In contrast, after HRW treatment, the 3×Tg-AD mice exhibited improvements in cognitive impairment. Escape latency was gradually shortened during the 5 days of spatial training in all of these mice (**Figure 1A** and **B**).

At 24 or 72 hours later, short- or long-term memory retention, respectively, was assessed using the probe trials. As shown in **Figure 1C** and **D**, the number of platform crossings and the amount of time mice spent in the target quadrant were much lower in the AD group than in the WT group ($P < 0.001$), indicating memory impairments in the 3×Tg-AD mice. Surprisingly, HRW-treated 3×Tg-AD mice demonstrated noticeable increases in the number of platform crossings and the amount of time spent in the target quadrant ($P < 0.05$ or $P < 0.01$, *vs*. AD group). In particular, the long-term memory dysfunction of 3×Tg-AD mice was significantly improved by HRW.

In addition, to evaluate the anti-depression and anti-anxiety effects of HRW, the anxiety behaviors of mice were evaluated using the open-field test. Compared with WT mice, the number of grids crossed and the amount of rearing by the 3×Tg-AD mice were significantly lower, while defecation frequency was increased ($P < 0.001$). These findings demonstrate the typical depression- and anxiety-like symptoms of 3×Tg-AD mice. In contrast, HRW treatment improved these emotional disorders in 3×Tg-AD mice, with an increased frequency of grid crossings and rearing and a decreased frequency of defecation ($P < 0.05$; **Figure 1E**). The results of these behavioral tests indicate that HRW treatment ameliorates the spatial learning and cognitive impairments of 3×Tg-AD mice.

HRW prevents synaptic loss and neuronal damage in 3×Tg-AD mice

The effects of HRW on the hippocampal levels of typical synaptic markers (postsynaptic density protein 95 and synaptophysin) were evaluated. As shown in **Figure 2A** and **B**, the levels of these two synaptic proteins in 3×Tg-AD mice with HRW treatment reached or even exceeded those in the WT mice ($P < 0.05$), suggesting that HRW promotes the recovery of synaptic function in AD model mice.

Neuronal death leads to the collapse of neural networks and further contributes to memory and cognitive impairments in neurodegenerative diseases, including AD (Vilalta and Brown, 2018). Here, neuronal injury in the CA1, CA3, dentate gyrus, and cortex (Paxinos and Franklin, 2013) was analyzed by Nissl staining. As shown in **Figure 2C** and **D**, HRW treatment significantly increased the density and number of Nissl bodies in 3×Tg-AD mice ($P < 0.05$ or $P < 0.01$). Thus, our findings indicate that HRW protects synaptic proteins and reverses neuronal damage in 3×Tg-AD mice.

HRW suppresses Aβ production and deposition in the hippocampus of 3×Tg-AD mice

To investigate the effects of HRW on Aβ pathology, the hippocampal levels of APP, secreted soluble APP α (sAPPα), and β-site APP-cleaving enzyme 1 (BACE1/β-secretase) were measured (**Figure 3**). In the western blot analysis, the levels of APP were higher in 3×Tg-AD mice than in WT mice ($P < 0.05$), and were significantly reduced after HRW treatment ($P < 0.001$; **Figure 3A** and **B**). The BACE1 levels were also significantly

reduced after HRW treatment ($P < 0.001$).

We used an anti-Aβ (6E10) antibody to perform immunofluorescence staining of hippocampal sections (CA3 region) to study Aβ deposition (**Figure 3C**). The immunofluorescence-positive area of Aβ deposition in the 3×Tg-AD mouse hippocampus was markedly larger than that of WT mice ($P < 0.01$), and was significantly reduced after HRW administration ($P < 0.05$; **Figure 3C** and **D**). In addition, the decreased sAPPα levels in 3×Tg-AD mice were partially recovered by HRW treatment, suggesting a neuroprotective effect of hydrogen ($P < 0.05$; **Figure 3A** and **B**). Together, these results indicate that HRW treatment has an intervention effect on the proteolysis of APP and on Aβ formation and deposition.

HRW suppresses tau hyperphosphorylation and NFT formation in 3×Tg-AD mice

As shown in **Figure 4A** and **B**, HRW treatment significantly inhibited tau phosphorylation at Ser422 and Ser404 in 3×Tg-AD mice ($P < 0.05$). In addition, glycine silver-positive NFTs were significantly decreased in the CA3 region in the HRW-treated group compared with 3×Tg-AD mice ($P < 0.05$; **Figure 4C** and **D**). These results indicate that HRW treatment can reduce tau pathology, which may prevent synaptic and neuronal damage and memory deficits in AD mice.

HRW inhibits inflammation and transforms microglia in an anti-inflammatory direction in 3×Tg-AD mice

After the continuous administration of HRW for 7 months, levels of the pro-inflammatory factors interleukin-6 and interleukin-1β were decreased ($P < 0.05$ or $P < 0.01$) compared with the AD group, while levels of the anti-inflammatory factor chitinase 3-like protein 3 (Ym-1) were increased ($P < 0.01$; **Figure 5A** and **B**). Iba-1 and glial fibrillary acidic protein are the classic indicators of microglia and astrocyte activation, respectively. Further western blot and immunofluorescence experiments demonstrated that hydrogen had a regulatory effect on glial cells, including microglia and astrocytes (**Figure 5A** and **C–G**). By western blot analysis, the levels of microglia and astrocytes were increased in 3×Tg-AD mice compared with WT mice ($P < 0.01$ or $P < 0.05$), while HRW treatment significantly reduced the levels of these two glial cell types ($P < 0.01$ or $P < 0.05$; **Figure 5A** and **C**). In addition, the immunofluorescence-positive area of Iba-1 in the 3×Tg-AD mouse cortex was larger than that of WT mice ($P < 0.001$), and was significantly reduced after HRW treatment in both the cortex and DG ($P < 0.001$ or $P < 0.05$; **Figure 5D–G**). These findings indicate that HRW can reduce pro-inflammatory cytokine production and enhance the secretion of anti-inflammatory factors, thereby exerting anti-inflammatory effects.

HRW improves bioenergetics in the brains of 3×Tg-AD mice

We determined the levels of several proteins that are related to mitochondrial energetics (pyruvate dehydrogenase component α subunit [PDHE1α], cytochrome c oxidase [COX] IV, and NADH dehydrogenase subunit 1 [ND1]) to assess the effects of HRW on mitochondrial energy metabolism. By western blot, the levels of these proteins were markedly lower in 3×Tg-AD mice compared with WT mice ($P < 0.05$, $P < 0.01$, or $P < 0.001$; **Figure 6A** and **B**), indicating the typical impaired mitochondrial function and bioenergetic deficiency of AD. HRW treatment significantly increased the PDHE1α levels ($P < 0.05$). Similarly, ATP concentrations in the 3×Tg-AD mouse hippocampus were also increased by HRW treatment ($P < 0.05$; **Figure 6C**). In this study, HRW was shown to be effective in reducing metabolic dysfunction and neuroinflammation in AD by manipulating the bioenergetic pathway.

HRW regulates the gut microbiota of 3×Tg-AD mice

The bacterial 16S ribosomal RNA genes were extracted from intestinal samples of 10-month-old mice and sequenced. In terms of bacterial communities, the Chao1 index was significantly smaller in 3×Tg-AD mice than in WT mice ($P < 0.01$), while HRW treatment increased the Chao1 index (**Figure 7A**). The diversification reflected in the Shannon index was similar to that in the Chao1 index (**Figure 7B**). The α diversity analysis (Chao1 and Shannon indices) revealed that the richness of bacterial species and diversity were lower in the intestines of 3×Tg-AD mice than in WT mice; HRW administration increased the richness and diversity of intestinal microflorae in 3×Tg-AD mice. The rarefaction curve also illustrated that HRW treatment recovered the richness and diversity of intestinal microbiota in the 3×Tg-AD mice (**Figure 7C**).

The Lachnospiraceae-NK4A136-group was the dominant bacterial type in all three groups of mice (**Figure 7D**), except for unclassified bacteria. Other genera with a relative abundance higher than 3% in each group are also depicted in **Figure 7D**, including Helicobacter in all three groups, Ruminococcaceae-UCG-014 in the WT and HRW-treated groups, and Alloprevotella in the 3×Tg-AD and HRW-treated groups. Compared with the WT mice, the relative abundances of Lachnospiraceae-NK4A136-group (7%) and Ruminococcaceae-NK4A136-group (< 4%, classified into "others") were lower in the 3×Tg-AD mice ($P < 0.05$; **Figure 7D** and **E**). Interestingly, the relative abundances of Lachnospiraceae-NK4A136-group and Ruminococcaceae-UCG-014 were enhanced after HRW treatment (**Figure 7D** and **E**), which may be one reason underlying the protective effects of HRW against the development of AD pathology. In addition, the abundance of Helicobacter in 3×Tg-AD mice was decreased from 6% to 4% by HRW treatment (**Figure 7E**). Together, our findings indicate a correlation between microbiota and the anti-AD effects of HRW administration. HRW treatment increased the abundance and diversity of intestinal microbiota in AD mice and regulated the relative abundance of specific flora, which may affect the pathological process of AD.

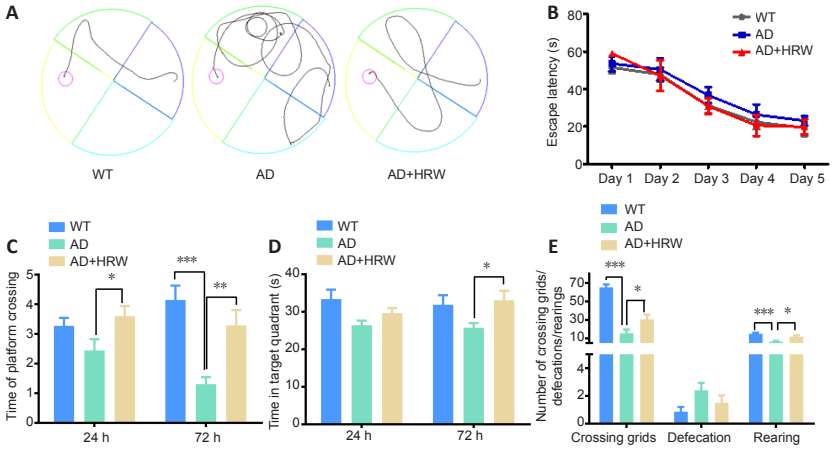

Figure 1 | HRW improves the cognitive impairment in 3×Tg-AD mice.
(A) Typical swimming traces in the probe test. The red circle indicates the hidden platform. The black line indicates the swimming trace. (B) Escape latency to find the hidden platform in the training task. (C) Number of crossings of the platform in the probe test. (D) Time spent in the target quadrant in the probe test. (E) Numbers of times the mice crossed the grids, defecated, and reared in the open-field test. Data are expressed as the mean ± SEM (n = 15 mice/group). *$P < 0.05$, **$P < 0.01$, ***$P < 0.001$ (one-way analysis of variance followed by Tukey's *post hoc* test). AD: Alzheimer's disease; HRW: hydrogen-rich water; WT: wild type.

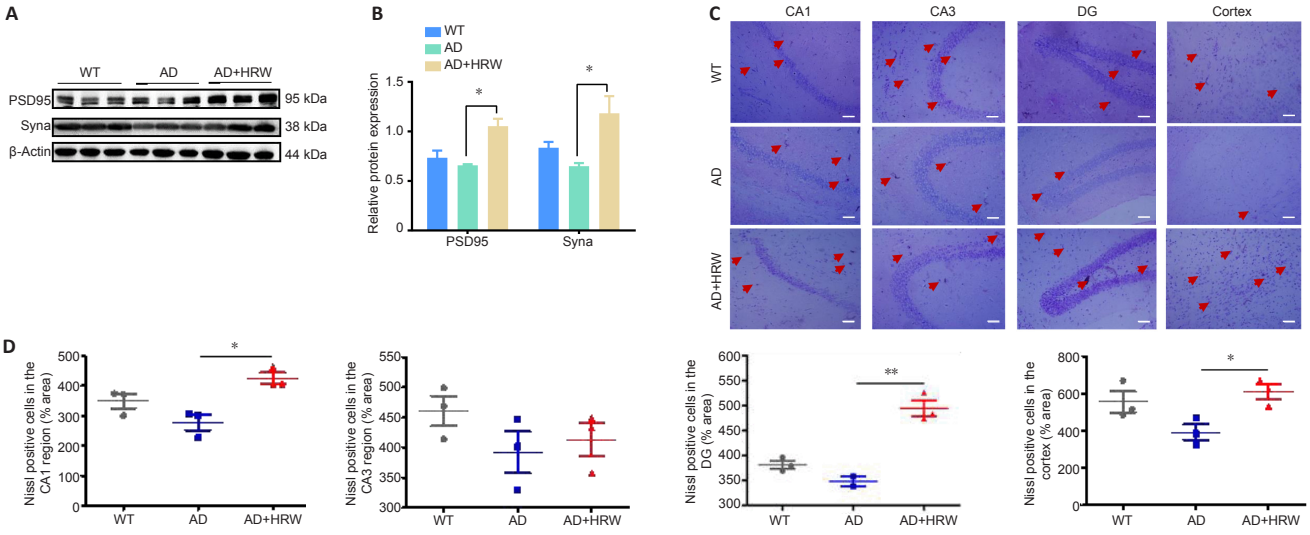

Figure 2 | HRW prevents synaptic loss and neuronal death in 3×Tg-AD mice.
(A) Effects of HRW on the hippocampal levels of PSD95 and Syna by western blot assay. (B) Quantification of PSD95 and Syna expression, normalized against β-actin. (C) Effects of HRW on the density and activity of neurons (arrows) in the CA1, CA3, DG, and cortex by Nissl staining. 3×Tg-AD mice exhibited decreased density and number of Nissl bodies; these were significantly recovered after HRW treatment. Scale bars: 50 μm. (D) Quantification of Nissl-positive neurons in the CA1, CA3, DG, and cortex. Data are expressed as the mean ± SEM (n = 3 mice/group). *P < 0.05, **P < 0.01 (one-way analysis of variance followed by Tukey's *post hoc* test). AD: Alzheimer's disease; DG: dentate gyrus; HRW: hydrogen-rich water; PSD95: postsynaptic density protein 95; Syna: synaptophysin; WT: wild type.

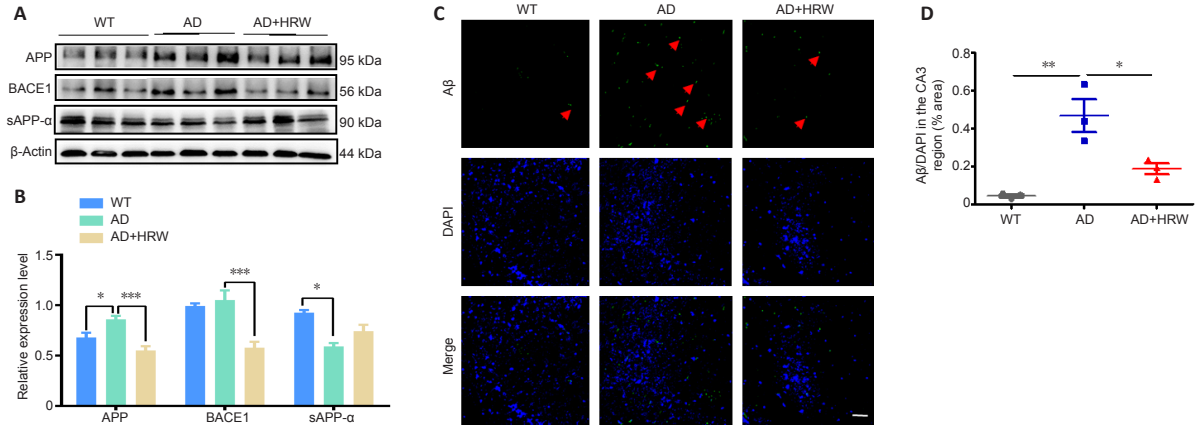

Figure 3 | HRW suppresses Aβ production and deposition in the hippocampus of 3×Tg-AD mice.
(A) Effects of HRW on hippocampal APP, sAPP-α, and BACE1 by western blot assay. (B) Quantification of APP, sAPP-α, and BACE1, normalized against β-actin. (C) Immunofluorescence images showing more Aβ (6E10) deposition (arrows) in the 3×Tg-AD mouse hippocampus compared with WT mice; this deposition was markedly reduced after HRW administration. Scale bar: 20 μm. (D) Quantification of Aβ deposition in the CA3 region of the hippocampus. Data are expressed as the mean ± SEM (n = 3 mice/group). *P < 0.05, **P < 0.01, ***P < 0.001 (one-way analysis of variance followed by Tukey's *post hoc* test). AD: Alzheimer's disease; APP: amyloid precursor protein; BACE1: beta-site APP cleaving enzyme 1; DAPI: 4′,6-diamidino-2-phenylindole; HRW: hydrogen-rich water; sAPP-α: soluble amyloid precursor protein α; WT: wild type.

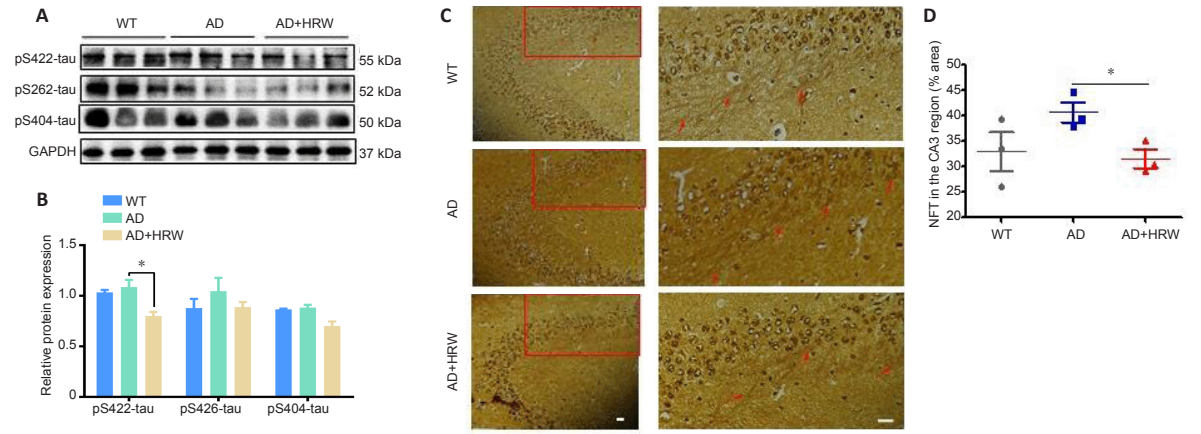

Figure 4 | HRW suppresses tau pathology in 3×Tg-AD mice.
(A) Effects of HRW on the hippocampal levels of pS422-, pS262-, and pS404-tau by western blot assay. (B) Quantification of pS422-, pS262-, and pS404-tau, normalized against GAPDH. (C) Glycine silver staining for NFTs in the mouse hippocampus, showing that the higher levels of NFTs (red arrows) in 3×Tg-AD mice were significantly reduced by HRW. Scale bar: 50 μm. (D) Quantification of NFTs in the hippocampal CA3 region. Data are expressed as the mean ± SEM (n = 3 mice/group). *P < 0.05 (one-way analysis of variance followed by Tukey's *post hoc* test). AD: Alzheimer's disease; GAPDH: glyceraldehyde-3-phosphate dehydrogenase; HRW: hydrogen-rich water; NFTs: neurofibrillary tangles; WT: wild type.

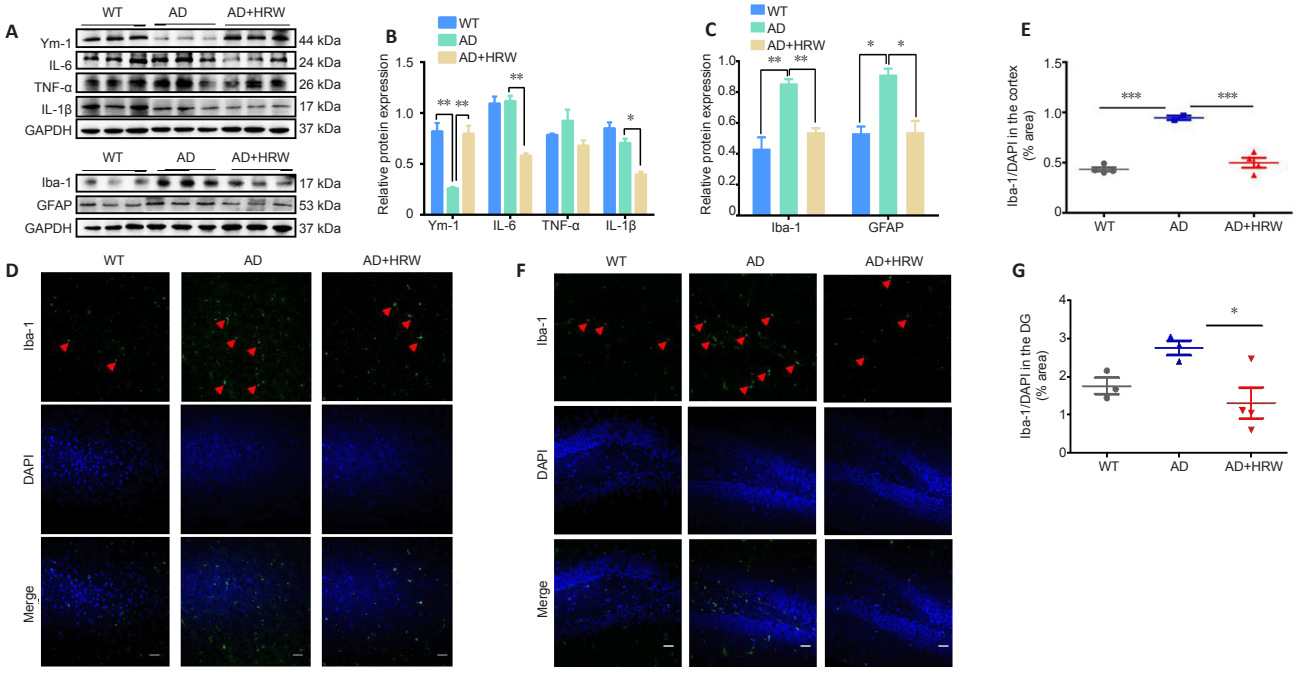

Figure 5 | Effects of HRW treatment on inflammation in the 3×Tg-AD mice.
(A) Effects of HRW on the hippocampal levels of Ym-1, IL-6, TNF-α, IL-1β, Iba-1, and GFAP in mice. (B, C) Quantification of Ym-1, IL-6, TNF-α, IL-1β, Iba-1, and GFAP, normalized against GAPDH. (D, F) The deposition of Iba-1 in the cortex (D) and hippocampal DG (F) was detected by immunofluorescence, and the overactivation of microglia in AD mice was clearly inhibited by HRW. Arrows indicate active Iba-1 (microglia). Scale bars: 50 μm. (E, G) Quantification of Iba-1 deposition in the cortex and hippocampal DG (G). Data are expressed as the mean ± SEM (n = 3 mice/group). *P < 0.05, **P < 0.01, ***P < 0.001 (one-way analysis of variance followed by Tukey's *post hoc* test). AD: Alzheimer's disease; DAPI: 4′,6-diamidino-2-phenylindole; DG: dentate gyrus; GAPDH: glyceraldehyde-3-phosphate dehydrogenase; GFAP: glial fibrillary acidic protein; HRW: hydrogen-rich water; Iba-1: ionized calcium-binding adapter molecule 1; IL-1β: interleukin-1β; IL-6: interleukin-6; TNF-α: tumor necrosis factor-α; WT: wild type; Ym-1: chitinase 3-like protein 3.

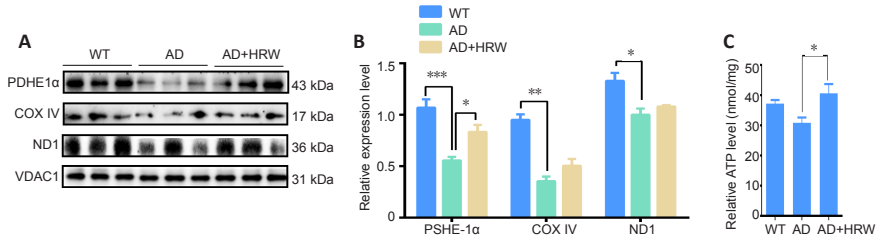

Figure 6 | Effects of HRW on bioenergetics in the hippocampus of 3×Tg-AD mice.
(A) Effects of HRW on the hippocampal levels of PDHE1α, COX IV, and ND1 by western blot assay. (B) Quantification of PDHE1α, COX IV, and ND1, normalized against the levels of VDAC1. (C) Quantitative analysis of the related ATP levels. Data are expressed as the mean ± SEM (n = 3 mice/group). *P < 0.05, **P < 0.01, ***P < 0.001 (one-way analysis of variance followed by Tukey's *post hoc* test). AD: Alzheimer's disease; COX IV: cytochrome C oxidase subunit IV; HRW: hydrogen-rich water; ND1: NADH-ubiquinone oxidoreductase chain 1; PDHE1α: α-subunit of pyruvate dehydrogenase; VDAC1: voltage-dependent anion channel 1; WT: wild type.

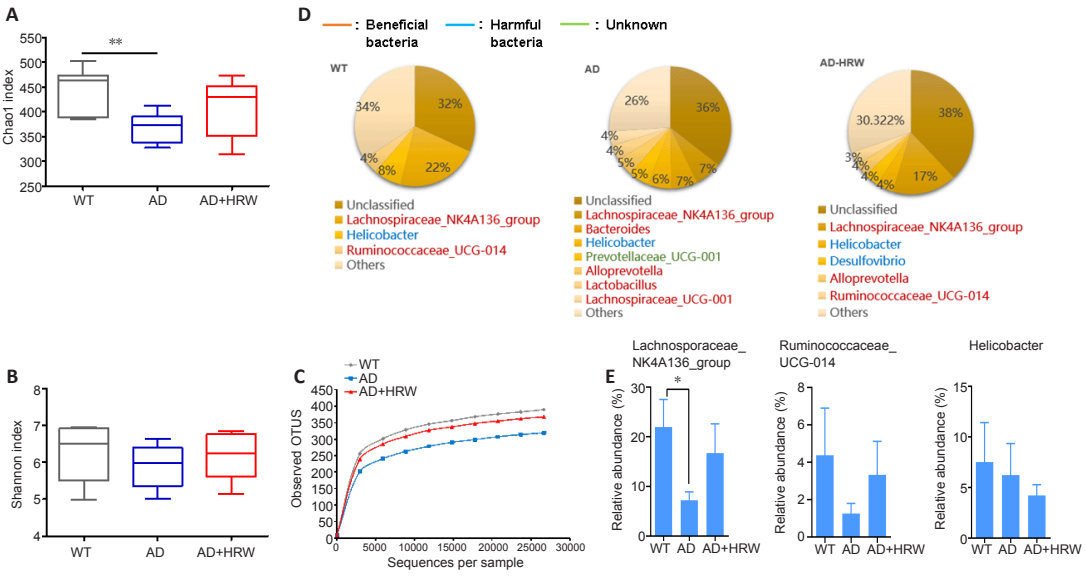

Figure 7 | Effects of HRW on gut microbiota in 3×Tg-AD mice.
(A–D) 16s ribosomal RNA gene sequencing showed changes to microbial diversity in mice, including in the box diagrams of Chao1 (A), Shannon diversity (B), the rarefaction curve (C), and the relative abundances of the main species at genus level (D). (E) The relative abundance of Lachnospiraceas_NK4A136_ group, Ruminococcaceae_ UCG-014, and Helicobacter in the three groups. Data are expressed as the mean ± SEM (n = 6 mice/group). *P < 0.05, **P < 0.01 (one-way analysis of variance followed by Tukey's *post hoc* test). AD: Alzheimer's disease; HRW: hydrogen-rich water, WT: wild type.

Discussion

The synapse is the basic unit for building neural networks in the brain (Vilalta and Brown, 2018). Aβ oligomers, phosphorylated tau, and oxidative stress all contribute to synaptic deficits, which are regarded as an early event of AD (Hong et al., 2016; Forner et al., 2017; Batista et al., 2018; Rice et al., 2019). In the present study, HRW treatment repaired the loss of synapses and neuronal damage in an AD mouse model. As reported previously, damage by reactive oxygen species contributes to the important neuropathological hallmarks of AD, including synaptic deficits and neuronal death (Rai et al., 2014; Deas et al., 2016; Angelova and Abramov, 2018). Thus, we hypothesize that hydrogen reduces the overproduction of reactive oxygen species, exerts further protection to synapses and neurons, and thus restores cognitive functions in AD.

Aβ is generated by the sequential proteolysis of APP by β- and γ-secretases (Allsop et al., 1988; Billings et al., 2005). $A\beta_{1-40}$ is the most abundant form of Aβ species (about 80–90% of all Aβ), whereas $A\beta_{1-42}$ (about 5–10% of all Aβ) is the main form that results in synaptic damage and neuronal death in the AD brain (Bozso et al., 2010). APP is cleaved by α- and γ-secretases to produce sAPPα through the non-amyloidogenic pathway. sAPPα is reported to have a variety of neuroprotective effects (Kojro et al., 2001; Selkoe and Schenk, 2003). In the current study, HRW treatment significantly decreased the levels of APP and Aβ in 3×Tg-AD mice, but increased sAPPα levels, suggesting that HRW has an intervention effect on the proteolysis of APP and on Aβ formation and deposition.

Tau is a microtubule-associated protein (Roberson et al., 2011; Guo et al., 2017). However, under pathological conditions, hyperphosphorylated tau disassociates from microtubules and assembles into NFTs (Congdon and Sigurdsson, 2018; Lowe et al., 2018), which are a critical pathological marker of AD (Spires-Jones et al., 2017; Villemagne et al., 2018). Tau and phosphorylated tau (pTau) have attracted considerable attention in recent years in terms of mechanism studies and drug discovery for AD. We revealed that HRW treatment reduced tau pathology, which may prevent synaptic and neuronal damage and memory deficits in AD mice.

Increasing evidence indicates that neuroinflammation is characteristic of AD. Inflammation is not only the main pathophysiological mechanism of Aβ production and senile plaque formation, but it is also a main factor in tau hyperphosphorylation, NFT formation, neuronal degeneration, and acetylcholine decline (Billings et al., 2005; Iketani and Ohsawa, 2017; Yang et al., 2018; Du et al., 2021). Inflammation disrupts synaptic plasticity as a direct driver of cognitive impairment in AD (Hong et al., 2016). Microglia and astrocytes are the main cell types involved in inflammatory responses of the central nervous system, which are extensively activated in AD brains (Heneka et al., 2015). At present, most treatments of large-scale anti-inflammatory drugs for AD deliver no significant improvement. Although some non-steroidal anti-inflammatory drugs have provided some improvement in AD symptoms in clinical trials, the overall significance is not great (Daniels et al., 2016; Sehajpal et al., 2018). Recently, molecular hydrogen has been reported to exhibit anti-inflammatory effects in many studies (Kura et al., 2019). In the current study, we observed that an anti-inflammatory role of hydrogen also existed in 3×Tg-AD mice. The inflammatory and anti-inflammatory factors that we detected, which are mainly produced and released by activated microglia, are thought to play important roles in AD pathogenesis, and lead to neuronal damage, apoptosis, and immune modulation. Activated microglia include classical inflammatory (M1) phenotypes and alternatively activated (M2) phenotypes (Kabba et al., 2018). M1 microglia produce and release destructive pro-inflammatory cytokines (Kumar et al., 2016); in contrast, M2 microglia express anti-inflammatory factors (Jha et al., 2016). Our results indicate that hydrogen may inhibit the excessive activation of microglia, transforming them in an anti-inflammatory direction (i.e., to M2 phenotypes).

Bioenergetic deficits have been regarded as a major contributor to cognitive decline and memory deficits (Su et al., 2014; Zhou et al., 2018; Filippov et al., 2021). The bioenergy hypothesis proposes events ranging from metabolic defects to aging and neurodegeneration. Loss of mitochondrial bioenergetics in AD leads to the decreased activity of relevant enzymes, which causes a reduction in the electron transport chain as well as energy (i.e., ATP) depletion (Ohno et al., 2012; Sheng and Cai, 2012; Su et al., 2014; Park et al., 2018; Zhou et al., 2018; Kempuraj et al., 2020). Pyruvate dehydrogenase complex is a key enzyme in aerobic carbohydrate metabolism (Zhong et al., 2015) whose deficiency is known to cause severe metabolic and neurodegenerative diseases (Zhou et al., 2018). Mitochondrial COX, a multimeric complex that is the last enzyme of the respiratory chain, is essential for aerobic energy generation in the form of ATP (Su et al., 2014; Kocha et al., 2015). NADH is a part of mitochondrial complex 1, which is the initial enzyme of the mitochondrial respiratory chain. Some previous research has suggested that inflammatory signals result in the enhanced phosphorylation of mitochondrial targets, including COX, leading to the inhibition of mitochondrial function, reduction of mitochondrial membrane potential, and energy failure (Zhong et al., 2016; Nishida and Otsu, 2017; Tilg et al., 2017; Biczo et al., 2018; Li et al., 2018). Moreover, mitochondrial dysfunction can also cause neuroinflammation (Zhou et al., 2018). In the present study, hydrogen was effective in reducing metabolic dysfunction and neuroinflammation in AD by manipulating the bioenergetic pathway.

A mounting number of studies have reported that microbiota, which live in symbiosis with animals, are a very important factor influencing the health of the host (Kabba et al., 2018; Yao and Zu, 2020). The gut microbiota integrate into the microbiota-gut-brain axis to regulate brain function and behavior (Valles-Colomer et al., 2019), and a correlation analysis has revealed that gut microbial metabolites are associated with AD (MahmoudianDehkordi et al., 2019; Tran et al., 2019). A variety of factors, including diet, can cause changes in gut microbiota and gut physiology. Here, we further investigated whether HRW may interfere with the gut microbiota of AD mice.

Previous studies have shown that Lachnospiraceae-NK4A136-group and Ruminococcaceae-UCG-014 are beneficial bacteria. Lachnospiraceae-NK4A136-group belongs to the family of Lachnospiraceae, which is thought to be relevant for the metabolism of carbohydrates into short-chain fatty acids that can be used by the host for energy (Manuel et al., 2019; Wang et al., 2019). Helicobacter pillory is related to gastritis and is a causative agent of gastric and duodenal ulcers (Albaret et al., 2020). The relative abundance of the Lachnospiraceae-NK4A136-group may be associated with increased intestinal mucosal permeability in patients with depression (Cheng et al., 2018). Ruminococcaceae-UCG-014, which belongs to the family of Ruminococcaceae, is regarded as a special functional microflora that can modulate the metabolism of host amino acids. It has great regulatory potential for persistent mental illnesses, such as mental state wilting and drowsiness (Gopalakrishnan et al., 2018). Thus, the decreased relative abundance of these two beneficial bacteria in the intestines of 3×Tg-AD mice may be associated with declined metabolic capacity, altered mental state, depression-like behavior, and wilting in 3×Tg-AD mice.

Some limitations of the study should be noted. First, young mice were subjected to long-term treatment of single-dose HRW. This study therefore suggests more of a preventative effect rather than a therapeutic effect of HRW on AD.

Furthermore, we were unable to identify whether the effect was dose-dependent. Second, the current study did not provide any information about the specific receptors/enzymes or cellular pathways on which HRW might act during neuroprotection. This should be considered in a future study.

In conclusion, a strong relationship between inflammation and the pathogenesis of AD has been demonstrated in numerous studies. As a novel and innovative therapeutic treatment, hydrogen may be developed as a potential therapy to treat diverse inflammatory diseases, including AD. In the current study, 3×Tg-AD mice were treated with HRW, which reversed cognitive impairment, prevented synaptic loss and neuronal death, inhibited Aβ generation and deposition, and reduced tau hyperphosphorylation and NFTs. We further demonstrated that HRW treatment exerted anti-inflammatory effects that were accompanied by improved bioenergetics and gut microbiota regulation in AD model mice. These findings demonstrate the encouraging potential of hydrogen as a therapeutic and prophylactic agent for neurodegenerative diseases, and suggest a new direction for AD treatment in the future.

Acknowledgments: *We thank Beijing Vitality Hydrogen Source Beverage Ltd. for providing the hydrogen-rich water.*
Author contributions: *Study conception and design: YTL, QQS, LZ, QJH, QL, XBD; experiment implementation: YTL, QQS, LZ, CPY, ZJH, XXL; data analysis: QQS, LZ; manuscript draft: YTL, QQS, LZ. All authors read and approved the final manuscript.*
Conflicts of interest: *The authors declare no conflicts of interest.*
Financial support: *This study was supported by the National Natural Science Foundation of China, No. 21771126 (to XBD); and the Shenzhen Bureau of Science, Technology and Information of China, No. JCYJ20180305124000597 (to XBD). The funding sources had no role in study conception and design, data analysis or interpretation, paper writing or deciding to submit this paper for publication.*
Institutional review board statement: *This study was approved by the Animal Ethics and Welfare Committee of Shenzhen University (approval No. AEWC-20140615-002) on June 15, 2014.*
Copyright license agreement: *The Copyright License Agreement has been signed by all authors before publication.*
Data sharing statement: *Datasets analyzed during the current study are available from the corresponding author on reasonable request.*
Plagiarism check: *Checked twice by iThenticate.*
Peer review: *Externally peer reviewed.*

Open peer reviewer: *Ahmed Abdel-Zaher, Assiut University, Egypt.*
Additional files:
Additional Table 1: *Antibody information.*
Additional file 1: *Original data of the experiment.*

References

Albaret G, Sifré E, Floch P, Laye S, Aubert A, Dubus P, Azzi-Martin L, Giese A, Salles N, Mégraud F, Varon C, Lehours P, Roubaud-Baudron C (2020) Alzheimer's disease and helicobacter pylori infection: inflammation from stomach to brain? J Alzheimers Dis 73:801-809.

Allsop D, Wong CW, Ikeda S, Landon M, Kidd M, Glenner GG (1988) Immunohistochemical evidence for the derivation of a peptide ligand from the amyloid beta-protein precursor of Alzheimer disease. Proc Natl Acad Sci U S A 85:2790-2794.

Angelova PR, Abramov AY (2018) Role of mitochondrial ROS in the brain: from physiology to neurodegeneration. FEBS Lett 592:692-702.

Batista AF, Forny-Germano L, Clarke JR, Lyra ESNM, Brito-Moreira J, Boehnke SE, Winterborn A, Coe BC, Lablans A, Vital JF, Marques SA, Martinez AM, Gralle M, Holscher C, Klein WL, Houzel JC, Ferreira ST, Munoz DP, De Felice FG (2018) The diabetes drug liraglutide reverses cognitive impairment in mice and attenuates insulin receptor and synaptic pathology in a non-human primate model of Alzheimer's disease. J Pathol 245:85-100.

Biczo G, Vegh ET, Shalbueva N, Mareninova OA, Elperin J, Lotshaw E, Gretler S, Lugea A, Malla SR, Dawson D, Ruchala P, Whitelegge J, French SW, Wen L, Husain SZ, Gorelick FS, Hegyi P, Rakonczay Z, Jr., Gukovsky I, Gukovskaya AS (2018) Mitochondrial dysfunction, through impaired autophagy, leads to endoplasmic reticulum stress, deregulated lipid metabolism, and pancreatitis in animal models. Gastroenterology 154:689-703.

Billings LM, Oddo S, Green KN, McGaugh JL, LaFerla FM (2005) Intraneuronal Abeta causes the onset of early Alzheimer's disease-related cognitive deficits in transgenic mice. Neuron 45:675-688.

Bozso Z, Penke B, Simon D, Laczkó I, Juhász G, Szegedi V, Kasza A, Soós K, Hetényi A, Wéber E, Tóháti H, Csete M, Zarándi M, Fülöp L (2010) Controlled in situ preparation of A beta(1-42) oligomers from the isopeptide "iso-A beta(1-42)", physicochemical and biological characterization. Peptides 31:248-256.

Cheng D, Chang H, Ma S, Guo J, She G, Zhang F, Li L, Li X, Lu Y (2018) Tiansi liquid modulates gut microbiota composition and tryptophan¯kynurenine metabolism in rats with hydrocortisone-induced depression. Molecules 23:2832.

Congdon EE, Sigurdsson EM (2018) Tau-targeting therapies for Alzheimer disease. Nat Rev Neurol 14:399-415.

Corpas FJ, González-Gordo S, Cañas A, Palma JM (2019) Nitric oxide and hydrogen sulfide in plants: which comes first? J Exp Bot 70:4391-4404.

Daniels MJ, Rivers-Auty J, Schilling T, Spencer NG, Watremez W, Fasolino V, Booth SJ, White CS, Baldwin AG, Freeman S, Wong R, Latta C, Yu S, Jackson J, Fischer N, Koziel V, Pillot T, Bagnall J, Allan SM, Paszek P, et al. (2016) Fenamate NSAIDs inhibit the NLRP3 inflammasome and protect against Alzheimer's disease in rodent models. Nat Commun 7:12504.

Deas E, Cremades N, Angelova PR, Ludtmann MH, Yao Z, Chen S, Horrocks MH, Banushi B, Little D, Devine MJ, Gissen P, Klenerman D, Dobson CM, Wood NW, Gandhi S, Abramov AY (2016) Alpha-synuclein oligomers interact with metal ions to induce oxidative stress and neuronal death in Parkinson's disease. Antioxid Redox Signal 24:376-391.

Du YH, Sun Y, Yang RY, Wang LY, Cai M (2021) Mechanisms of neuroinflammation in mild cognitive impairment. Zhongguo Zuzhi Gongcheng Yanjiu 25:4743-4749.

Fang EF, Hou Y, Palikaras K, Adriaanse BA, Kerr JS, Yang B, Lautrup S, Hasan-Olive MM, Caponio D, Dan X, Rocktäschel P, Croteau DL, Akbari M, Greig NH, Fladby T, Nilsen H, Cader MZ, Mattson MP, Tavernarakis N, Bohr VA (2019) Mitophagy inhibits amyloid-β and tau pathology and reverses cognitive deficits in models of Alzheimer's disease. Nat Neurosci 22:401-412.

Filippov MA, Tatarnikova OG, Pozdnyakova NV, Vorobyov VV (2021) Inflammation/bioenergetics-associated neurodegenerative pathologies and concomitant diseases: a role of mitochondria targeted catalase and xanthophylls. Neural Regen Res 16:223-233.

Forner S, Baglietto-Vargas D, Martini AC, Trujillo-Estrada L, LaFerla FM (2017) Synaptic impairment in Alzheimer's disease: a dysregulated symphony. Trends Neurosci 40:347-357.

Frere S, Slutsky I (2018) Alzheimer's disease: from firing instability to homeostasis network collapse. Neuron 97:32-58.

Gopalakrishnan V, Spencer CN, Nezi L, Reuben A, Andrews MC, Karpinets TV, Prieto PA, Vicente D, Hoffman K, Wei SC, Cogdill AP, Zhao L, Hudgens CW, Hutchinson DS, Manzo T, Petaccia de Macedo M, Cotechini T, Kumar T, Chen WS, Reddy SM, et al. (2018) Gut microbiome modulates response to anti-PD-1 immunotherapy in melanoma patients. Science 359:97-103.

Gray SC, Kinghorn KJ, Woodling NS (2020) Shifting equilibriums in Alzheimer's disease: the complex roles of microglia in neuroinflammation, neuronal survival and neurogenesis. Neural Regen Res 15:1208-1219.

Guo T, Noble W, Hanger DP (2017) Roles of tau protein in health and disease. Acta Neuropathol 133:665-704.

Hammer C, Stepniak B, Schneider A, Papiol S, Tantra M, Begemann M, Sirén AL, Pardo LA, Sperling S, Mohd Jofrry S, Gurvich A, Jensen N, Ostmeier K, Lühder F, Probst C, Martens H, Gillis M, Saher G, Assogna F, Spalletta G, et al. (2014) Neuropsychiatric disease relevance of circulating anti-NMDA receptor autoantibodies depends on blood-brain barrier integrity. Mol Psychiatry 19:1143-1149.

Heneka MT, Carson MJ, El Khoury J, Landreth GE, Brosseron F, Feinstein DL, Jacobs AH, Wyss-Coray T, Vitorica J, Ransohoff RM, Herrup K, Frautschy SA, Finsen B, Brown GC, Verkhratsky A, Yamanaka K, Koistinaho J, Latz E, Halle A, Petzold GC, et al. (2015) Neuroinflammation in Alzheimer's disease. Lancet Neurol 14:388-405.

Hong S, Beja-Glasser VF, Nfonoyim BM, Frouin A, Li S, Ramakrishnan S, Merry KM, Shi Q, Rosenthal A, Barres BA, Lemere CA, Selkoe DJ, Stevens B (2016) Complement and microglia mediate early synapse loss in Alzheimer mouse models. Science 352:712-716.

Iida A, Nosaka N, Yumoto T, Knaup E, Naito H, Nishiyama C, Yamakawa Y, Tsukahara K, Terado M, Sato K, Ugawa T, Nakao A (2016) The Clinical application of hydrogen as a medical treatment. Acta Med Okayama 70:331-337.

Iketani M, Ohsawa I (2017) Molecular hydrogen as a neuroprotective agent. Curr Neuropharmacol 15:324-331.

Jack CR, Jr., Bennett DA, Blennow K, Carrillo MC, Dunn B, Haeberlein SB, Holtzman DM, Jagust W, Jessen F, Karlawish J, Liu E, Molinuevo JL, Montine T, Phelps C, Rankin KP, Rowe CC, Scheltens P, Siemers E, Snyder HM, Sperling R (2018) NIA-AA Research Framework: Toward a biological definition of Alzheimer's disease. Alzheimers Dement 14:535-562.

Jha MK, Lee WH, Suk K (2016) Functional polarization of neuroglia: Implications in neuroinflammation and neurological disorders. Biochem Pharmacol 103:1-16.
Kabba JA, Xu Y, Christian H, Ruan W, Chenai K, Xiang Y, Zhang L, Saavedra JM, Pang T (2018) Microglia: housekeeper of the central nervous system. Cell Mol Neurobiol 38:53-71.
Kempuraj D, Ahmed ME, Selvakumar GP, Thangavel R, Dhaliwal AS, Dubova I, Mentor S, Premkumar K, Saeed D, Zahoor H, Raikwar SP, Zaheer S, Iyer SS, Zaheer A (2020) Brain injury-mediated neuroinflammatory response and Alzheimer's disease. Neuroscientist 26:134-155.
Kocha KM, Reilly K, Porplycia DS, McDonald J, Snider T, Moyes CD (2015) Evolution of the oxygen sensitivity of cytochrome c oxidase subunit 4. Am J Physiol Regul Integr Comp Physiol 308:R305-320.
Kojro E, Gimpl G, Lammich S, Marz W, Fahrenholz F (2001) Low cholesterol stimulates the nonamyloidogenic pathway by its effect on the alpha-secretase ADAM 10. Proc Natl Acad Sci U S A 98:5815-5820.
Kumar A, Barrett JP, Alvarez-Croda DM, Stoica BA, Faden AI, Loane DJ (2016) NOX2 drives M1-like microglial/macrophage activation and neurodegeneration following experimental traumatic brain injury. Brain Behav Immun 58:291-309.
Kumar M, Sandhir R (2018) Hydrogen sulfide in physiological and pathological mechanisms in brain. CNS Neurol Disord Drug Targets 17:654-670.
Kura B, Bagchi AK, Singal PK, Barancik M, LeBaron TW, Valachova K, Šoltés L, Slezák J (2019) Molecular hydrogen: potential in mitigating oxidative-stress-induced radiation injury (1). Can J Physiol Pharmacol 97:287-292.
Li R, Xin T, Li D, Wang C, Zhu H, Zhou H (2018) Therapeutic effect of Sirtuin 3 on ameliorating nonalcoholic fatty liver disease: The role of the ERK-CREB pathway and Bnip3-mediated mitophagy. Redox Biol 18:229-243.
Lowe VJ, Wiste HJ, Senjem ML, Weigand SD, Therneau TM, Boeve BF, Josephs KA, Fang P, Pandey MK, Murray ME, Kantarci K, Jones DT, Vemuri P, Graff-Radford J, Schwarz CG, Machulda MM, Mielke MM, Roberts RO, Knopman DS, Petersen RC, et al. (2018) Widespread brain tau and its association with ageing, Braak stage and Alzheimer's dementia. Brain 141:271-287.
Lozupone C, Knight R (2005) UniFrac: a new phylogenetic method for comparing microbial communities. Appl Environ Microbiol 71:8228-8235.
MahmoudianDehkordi S, Arnold M, Nho K, Ahmad S, Jia W, Xie G, Louie G, Kueider-Paisley A, Moseley MA, Thompson JW, St John Williams L, Tenenbaum JD, Blach C, Baillie R, Han X, Bhattacharyya S, Toledo JB, Schafferer S, Klein S, Koal T, et al. (2019) Altered bile acid profile associates with cognitive impairment in Alzheimer's disease-An emerging role for gut microbiome. Alzheimers Dement 15:76-92.
Manuel CR, Latuga MS, Ashby CR, Jr., Reznik SE (2019) Immune tolerance attenuates gut dysbiosis, dysregulated uterine gene expression and high-fat diet potentiated preterm birth in mice. Am J Obstet Gynecol 220:596.e1-596.e28.
Markesbery WR (1997) Oxidative stress hypothesis in Alzheimer's disease. Free Radic Biol Med 23:134-147.
Mostafavi S, Gaiteri C, Sullivan SE, White CC, Tasaki S, Xu J, Taga M, Klein HU, Patrick E, Komashko V, McCabe C, Smith R, Bradshaw EM, Root DE, Regev A, Yu L, Chibnik LB, Schneider JA, Young-Pearse TL, Bennett DA, et al. (2018) A molecular network of the aging human brain provides insights into the pathology and cognitive decline of Alzheimer's disease. Nat Neurosci 21:811-819.
Nishida K, Otsu K (2017) Inflammation and metabolic cardiomyopathy. Cardiovasc Res 113:389-398.
Oddo S, Caccamo A, Kitazawa M, Tseng BP, LaFerla FM (2003) Amyloid deposition precedes tangle formation in a triple transgenic model of Alzheimer's disease. Neurobiol Aging 24:1063-1070.
Ohno K, Ito M, Ichihara M, Ito M (2012) Molecular hydrogen as an emerging therapeutic medical gas for neurodegenerative and other diseases. Oxid Med Cell Longev 2012:353152.
Ohta S (2015) Molecular hydrogen as a novel antioxidant: overview of the advantages of hydrogen for medical applications. Methods Enzymol 555:289-317.
Olas B (2017) Hydrogen sulfide as a "double-faced" compound: one with pro- and antioxidant effect. Adv Clin Chem 78:187-196.
Ozben T, Ozben S (2019) Neuro-inflammation and anti-inflammatory treatment options for Alzheimer's disease. Clin Biochem 72:87-89.
Park J, Wetzel I, Marriott I, Dréau D, D'Avanzo C, Kim DY, Tanzi RE, Cho H (2018) A 3D human triculture system modeling neurodegeneration and neuroinflammation in Alzheimer's disease. Nat Neurosci 21:941-951.
Paxinos G, Franklin KB (2013) The Mouse Brain in Stereotaxic Coordinates. San Diego: Elsevier.
Rai S, Kamat PK, Nath C, Shukla R (2014) Glial activation and post-synaptic neurotoxicity: the key events in streptozotocin (ICV) induced memory impairment in rats. Pharmacol Biochem Behav 117:104-117.
Rice HC, de Malmazet D, Schreurs A, Frere S, Van Molle I, Volkov AN, Creemers E, Vertkin I, Nys J, Ranaivoson FM, Comoletti D, Savas JN, Remaut H, Balschun D, Wierda KD, Slutsky I, Farrow K, De Strooper B, de Wit J (2019) Secreted amyloid-β precursor protein functions as a GABA(B)R1a ligand to modulate synaptic transmission. Science 363:eaao4827.
Roberson ED, Halabisky B, Yoo JW, Yao J, Chin J, Yan F, Wu T, Hamto P, Devidze N, Yu GQ, Palop JJ, Noebels JL, Mucke L (2011) Amyloid-β/Fyn-induced synaptic, network, and cognitive impairments depend on tau levels in multiple mouse models of Alzheimer's disease. J Neurosci 31:700-711.
Sehajpal S, Prasad DN, Singh RK (2018) Prodrugs of non-steroidal anti-inflammatory drugs (NSAIDs): a long march towards synthesis of safer NSAIDs. Mini Rev Med Chem 18:1199-1219.
Selkoe DJ, Schenk D (2003) Alzheimer's disease: molecular understanding predicts amyloid-based therapeutics. Annu Rev Pharmacol Toxicol 43:545-584.
Sheng ZH, Cai Q (2012) Mitochondrial transport in neurons: impact on synaptic homeostasis and neurodegeneration. Nat Rev Neurosci 13:77-93.
Shoji H, Takao K, Hattori S, Miyakawa T (2016) Age-related changes in behavior in C57BL/6J mice from young adulthood to middle age. Mol Brain 9:11.
Smith PK, Krohn RI, Hermanson GT, Mallia AK, Gartner FH, Provenzano MD, Fujimoto EK, Goeke NM, Olson BJ, Klenk DC (1985) Measurement of protein using bicinchoninic acid. Anal Biochem 150:76-85.
Spires-Jones TL, Attems J, Thal DR (2017) Interactions of pathological proteins in neurodegenerative diseases. Acta Neuropathol 134:187-205.
Su CH, McStay GP, Tzagoloff A (2014) Assembly of the rotor component of yeast mitochondrial ATP synthase is enhanced when Atp9p is supplied by Atp9p-Cox6p complexes. J Biol Chem 289:31605-31616.
Tilg H, Moschen AR, Roden M (2017) NAFLD and diabetes mellitus. Nat Rev Gastroenterol Hepatol 14:32-42.
Tran TTT, Corsini S, Kellingray L, Hegarty C, Le Gall G, Narbad A, Müller M, Tejera N, O'Toole PW, Minihane AM, Vauzour D (2019) APOE genotype influences the gut microbiome structure and function in humans and mice: relevance for Alzheimer's disease pathophysiology. FASEB J 33:8221-8231.
Valles-Colomer M, Falony G, Darzi Y, Tigchelaar EF, Wang J, Tito RY, Schiweck C, Kurilshikov A, Joossens M, Wijmenga C, Claes S, Van Oudenhove L, Zhernakova A, Vieira-Silva S, Raes J (2019) The neuroactive potential of the human gut microbiota in quality of life and depression. Nature microbiology 4:623-632.
Vilalta A, Brown GC (2018) Neurophagy, the phagocytosis of live neurons and synapses by glia, contributes to brain development and disease. FEBS J 285:3566-3575.
Villemagne VL, Doré V, Burnham SC, Masters CL, Rowe CC (2018) Imaging tau and amyloid-β proteinopathies in Alzheimer disease and other conditions. Nat Rev Neurol 14:225-236.
Wang S, Yang J, Zhang B, Zhang L, Wu K, Yang A, Li C, Wang Y, Zhang J, Qi D (2019) Potential link between gut microbiota and deoxynivalenol-induced feed refusal in weaned piglets. J Agric Food Chem 67:4976-4986.
Xie Y, Liu Q, Zheng L, Wang B, Qu X, Ni J, Zhang Y, Du X (2018) Se-methylselenocysteine ameliorates neuropathology and cognitive deficits by attenuating oxidative stress and metal dyshomeostasis in Alzheimer model mice. Mol Nutr Food Res 62:e1800107.
Yang Y, Zhu Y, Xi X (2018) Anti-inflammatory and antitumor action of hydrogen via reactive oxygen species. Oncol Lett 16:2771-2776.
Yao K, Zu HB (2020) Microglial polarization: novel therapeutic mechanism against Alzheimer's disease. Inflammopharmacology 28:95-110.
Zhang L, Zhao P, Yue C, Jin Z, Liu Q, Du X, He Q (2019) Sustained release of bioactive hydrogen by Pd hydride nanoparticles overcomes Alzheimer's disease. Biomaterials 197:393-404.
Zhang X, Bian JS (2014) Hydrogen sulfide: a neuromodulator and neuroprotectant in the central nervous system. ACS Chem Neurosci 5:876-883.
Zhong Y, Huang R, Li X, Xu R, Zhou F, Wang J, Fan H, Goscinski M, Zhang M, Wen JG, Nesland JM, Suo Z (2015) Decreased expression of PDHE1α predicts worse clinical outcome in esophageal squamous cell carcinoma. Anticancer Res 35:5533-5538.
Zhong Z, Umemura A, Sanchez-Lopez E, Liang S, Shalapour S, Wong J, He F, Boassa D, Perkins G, Ali SR, McGeough MD, Ellisman MH, Seki E, Gustafsson AB, Hoffman HM, Diaz-Meco MT, Moscat J, Karin M (2016) NF-κB restricts inflammasome activation via elimination of damaged mitochondria. Cell 164:896-910.
Zhou Z, Austin GL, Young LEA, Johnson LA, Sun R (2018) Mitochondrial metabolism in major neurological diseases. Cells 7:229.

P-Reviewer: Abdel-Zaher A; C-Editor: Zhao M; S-Editors: Yu J, Li CH; L-Editors: Gardner B, Yu J, Song LP; T-Editor: Jia Y

Additional Table 1 Antibody information

Antibody	Host	Application	Source	Dilutions
PSD95	Rabbit	WB	Abcam (Cambridge, MA, USA)	1:1000
Syna	Rabbit	WB	Abcam	1:50000
APP	Rabbit	WB	Abcam	1:20000
Bace-1	Rabbit	WB	Abcam	1:3000
sAPP-α	Rabbit	WB	Biolegend (San Diego, CA, USA)	1:5000
Aβ (6E10)	Mouse	IF	Biolegend	1:5000
pS262-tau	Rabbit	WB	Abcam	1:300
pS422-tau	Rabbit	WB	Abcam	1:15000
pS404-tau	Rabbit	WB	Abcam	1:1000
Ym-1	Rabbit	WB	Abcam	1:900
IL-6	Rabbit	WB	Abcam	1:1000
TNF-α	Rabbit	WB	Abcam	1:1000
IL-1β	Rabbit	WB	Abcam	1:4000
Iba-1	Rabbit	WB/IF	Abcam	1:1000/1:100
GFAP	Rabbit	WB	Abcam	1:10000
PDHE1α	Rabbit	WB	Abcam	1:2500
COX IV	Rabbit	WB	Abcam	1:2000
ND1	Rabbit	WB	Abcam	1:10000
β-Actin	Mouse	WB	Proteintech (Chicago, IL, USA)	1:25000
GAPDH	Mouse	WB	Abways (Beijing, China)	1:20000
VDAC1	Rabbit	WB	Abcam	1:10000
Goat anti-mouse IgG-horseradish peroxidase	Goat	WB	Abmart (Shanghai, China)	1:8000
Goat anti-rabbit IgG-horseradish peroxidase	Goat	WB	Abmart	1:8000
DyLight488 goat anti-mouse IgG	Goat	IF	Multi Sciences (Hangzhou, China) Multi Sciences	1:500
DyLight488 goat anti-rabbit IgG	Goat	IF		1:500

APP: Amyloid precursor protein; Aβ (6E10): β-amyloid; Bace-1: beta-site APP cleaving enzyme 1; COX IV: Cytochrome C oxidase subunit IV; GAPDH: glyceraldehyde-3-phosphate dehydrogenase; GFAP: glial fibrillary acidic protein; Iba-1: ionized calcium binding adapter molecule 1; IF: immunofluorescence; IL-1β: interleukin-1β; IL-6: interleukin-6; ND1: NADH-ubiquinone oxidoreductase chain 1; PDHE1α: α-subunit of pyruvate dehydrogenase; PSD95: postsynaptic density protein 95; sAPP-α: soluble amyloid precursor protein α; Syna: synaptophysin; TNF-α: tumor necrosis factor-α; VDAC1: voltage dependent anion channel 1; WB: Western blot; Ym-1: molecule chitinase 3 like protein 3.